Chronicling changes in the somatosensory neurons after peripheral nerve injury

Shrinivasan Raghuraman[a,1], Jennifer Y. Xie[b,c,1], Mario J. Giacobassi[a], Jortan O. Tun[a], Kevin Chase[a], Dong Lu[b], Russell W. Teichert[a], Frank Porreca[b], and Baldomero M. Olivera[a,2]

[a]School of Biological Sciences, University of Utah, Salt Lake City, UT 84112; [b]Department of Pharmacology, University of Arizona Health Sciences, Tucson, AZ 85724; and [c]Department of Basic Sciences, New York Institute of Technology College of Osteopathic Medicine at Arkansas State University, Jonesboro, AR 72467

Contributed by Baldomero M. Olivera, July 27, 2020 (sent for review December 27, 2019; reviewed by Armen N. Akopian and George Kanianthara Chandy)

Current drug discovery efforts focus on identifying lead compounds acting on a molecular target associated with an established pathological state. Concerted molecular changes that occur in specific cell types during disease progression have generally not been identified. Here, we used constellation pharmacology to investigate rat dorsal root ganglion neurons using two models of peripheral nerve injury: chronic constriction injury (CCI) and spinal nerve ligation (SNL). In these well-established models of neuropathic pain, we show that the onset of chronic pain is accompanied by a dramatic, previously unreported increase in the number of bradykinin-responsive neurons, with larger increases observed after SNL relative to CCI. To define the neurons with altered expression, we charted the temporal course of molecular changes following 1, 3, 6, and 14 d after SNL injury and demonstrated that specific molecular changes have different time courses during the progression to a pain state. In particular, ATP receptors upregulated on day 1 postinjury, whereas the increase in bradykinin receptors was gradual after day 3 postinjury. We specifically tracked changes in two subsets of neurons: peptidergic and nonpeptidergic nociceptors. Significant increases occurred in ATP responses in nAChR-expressing isolectin B4+ nonpeptidergic neurons 1 d postinjury, whereas peptidergic neurons did not display any significant change. We propose that remodeling of ion channels and receptors occurs in a concerted and cell-specific manner, resulting in the appearance of bradykinin-responsive neuronal subclasses that are relevant to chronic pain.

bradykinin | dorsal root ganglion | cell types | nerve injury | constellation pharmacology

Remarkable advances have been made in understanding the neural circuitry that underlies pain. In addition to defining the nociceptive circuitry by identifying the neurons that comprise these circuits, the cell-specific molecular changes that take place during the establishment of chronic pain states need to be systematically elucidated. This is a prerequisite for an integrated cellular and molecular framework for chronic pain. Analysis of changes in the functional expression of receptor constellations in different cell types can offer insights into which changes are relevant to pain pathology.

In this work, we demonstrate the application of constellation pharmacology (1) to monitor phenotypic changes that take place in populations of dorsal root ganglion (DRG) neurons as a chronic pain state is established. DRG contains many different classes of neurons that relay a variety of sensory information to higher centers in the brain (2). It remains unclear how different classes of DRG neurons respond to nerve injury. To address this, we used calcium imaging-based constellation pharmacology platform to uncover receptor constellations in different cell types. We monitored intracellular calcium responses elicited by rat DRG cells in response to the serial application of the following agonists: acetylcholine, ATP, bradykinin, menthol, allyl isothiocynate, and capsaicin. Some questions addressed in this work are: when chronic pain is established, what changes take place in the combinations of ion channels, and in receptors expressed in DRG neurons? How do these changes affect cellular phenotypes? Are some of these molecular changes that take place in these neurons coordinated? What molecular changes accompany the progression to neuropathic pain states?

For the present study, we have used two rodent models of neuropathic pain: Chronic Constriction Injury (CCI) and Spinal Nerve Ligation (SNL) of the rat (3, 4). These are well-validated animal models for chronic pain that recapitulate human clinical conditions associated with peripheral nerve injury, including surgical procedures such as thoracotomy, mastectomy that often result in chronic pain associated with peripheral nerve damage. Chronic pain, like other neurological disorders, has a spectrum of associated molecular changes depending on the pathological trigger (5). The results with the CCI and SNL rats suggest that the onset of chronic pain is accompanied by an increase in the frequency of neurons responding to bradykinin, with more dramatic effects observed in the SNL model compared to CCI. It is well known that bradykinin potently elicits pain, and there are widespread observations in the literature suggesting that bradykinin is linked in its activity to a number of ion channels and receptors expressed in sensory neurons (6). The binding of bradykinin to its GPCR (in particular bradykinin B2 receptor) results in an increase in cytosolic calcium mediated by intracellular stores. We have focused our analysis on DRG neurons that

Significance

In this work, cell-specific temporal changes that occur in DRG neurons after peripheral nerve injury were monitored. Altered responses of neurons to bradykinin, ATP, and acetylcholine were observed; three bradykinin responsive neuronal cell types appear that correlate with increased pain. The ability to temporally monitor cell-specific alterations in receptors and ion channels (termed as "Pigafetta Disease Chronicles") should make it possible to uncover cell type-specific disease-relevant alterations in membrane macromolecules and potentially identify drug targets whose function is required to establish a pathological state. This opens up the possibility of designing novel therapeutic interventions that do not merely treat disease symptoms but prevent a pathological state altogether.

Author contributions: S.R., J.Y.X., R.W.T., F.P., and B.M.O. designed research; S.R., J.Y.X., J.O.T., and D.L. performed research; S.R., J.Y.X., M.J.G., J.O.T., K.C., and B.M.O. analyzed data; and S.R. and B.M.O. wrote the paper.

Reviewers: A.N.A., University of Texas Health Sciences Center at San Antonio; and G.K.C., Nanyang Technological University.

The authors declare no competing interest.

[1]S.R. and J.Y.X. contributed equally to this work.

[2]To whom correspondence may be addressed. Email: olivera@biology.utah.edu.

This article contains supporting information online at https://www.pnas.org/lookup/suppl/doi:10.1073/pnas.1922618117/-/DCSupplemental.

First published October 5, 2020.

responded to the application of bradykinin. Constellation pharmacology allowed us to observe subsets of DRG neurons that are affected by the increase in bradykinin receptor expression and assess whether other changes in ion channel and receptor functions are also observed in these neurons. In addition, we performed phenotypic assessment of these bradykinin-responsive neurons with the progression of neuropathic pain following day 1, 3, 6, and 14 post-SNL injury.

We report a set of significant molecular changes in ATP, acetylcholine, bradykinin, and capsaicin responsive neurons that result in the appearance of subclasses of bradykinin-responsive DRG neurons as a consequence of CCI and SNL injury. Some of the changes appear to occur in a concerted manner (such as down-regulation of nAChR and up-regulation of ATP receptors), which suggests simultaneous downstream effects of the nerve injury on the constellations of ion channels and receptors in subsets of DRG neurons. These concerted changes raise the possibility of developing a complementary combination of therapeutic drugs to prevent, reverse, or inhibit the aberrant neuronal activity resulting from such concerted changes that accompany the progression to a pathological chronic pain state.

Results

CCI and SNL Injury Induced Changes to DRG Receptor Constellations. A primary culture of dissociated DRG cells from CCI- and SNL-operated animals was prepared and analyzed using constellation pharmacology. Seven pharmacological challenges were tested (acetylcholine, ATP, bradykinin, menthol, allyl isothiocyanate, capsaicin, and high extracellular K+). An increase in cytosolic calcium concentration, $[Ca]_i$, in response to the pharmacological challenge was monitored by fluorescence of the calcium-sensitive dye Fura 2 using two wavelengths.

The responses to the application of 30 mM $[K^+]_o$ and morphology of cells were used to differentiate neurons from non-neuronal cells. Fig. 1 summarizes the molecular changes following CCI and SNL injury. As shown in Fig. 1*A*, there was a decrease in the frequency of neurons responding to the application of acetylcholine ($P < 0.05$) and capsaicin ($P < 0.001$) in the ipsilateral CCI, and a significant increase in the frequency of neurons responding to ATP and bradykinin ($P < 0.001$). These observations align with previous studies performed on whole DRG (7–9). These changes were more dramatic in SNL-operated rats as shown in Fig. 1*B*. We have specifically investigated the increase in the frequency of DRG neurons that respond to bradykinin in the injured ipsilateral DRG neurons of the CCI- and SNL-operated rats. The diversity of response patterns to six pharmacological ligands is quantitated in *SI Appendix*, Table S1. For CCI trials, DRG neurons from 13 CCI-operated rats and 11 sham-operated rats were analyzed and, for SNL trials, neurons from 5 SNL-operated and 4 sham-operated rats were analyzed. Although there is some variation in the three uninjured DRG groups (contralateral CCI and ipsilateral and contralateral DRG from sham-operated animals), the data reveal a significant divergence in the frequency of cells responding to the pharmacological challenges in the ipsilateral CCI DRG neurons (*SI Appendix*, Table S1).

For the ease of understanding these datasets, we have grouped data obtained from uninjured DRG neurons (contralateral CCI, sham-operated ipsilateral, and contralateral DRG neurons) and labeled them as "CCI controls" and similarly grouped data obtained from uninjured DRG neurons from SNL-operated and sham-operated rats (SNL ipsilateral L4, SNL contralateral L4, SNL contralateral L5L6, sham-operated ipsilateral, and contralateral L4, L5, and L6) and labeled them as "SNL controls." As noted in *SI Appendix*, Table S1, there were no differences observed between uninjured DRG neurons in their responsiveness to the panel of pharmacological agents tested.

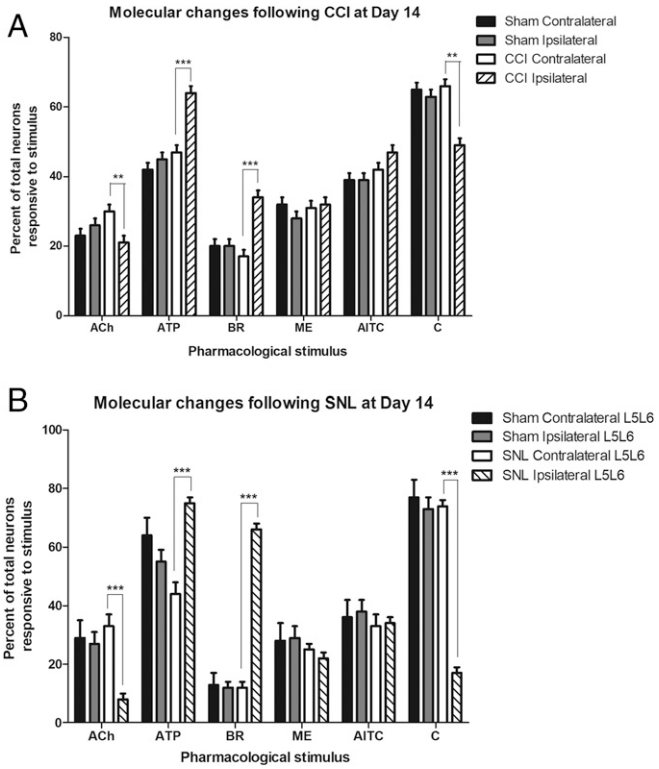

Fig. 1. Summary of profiling experiments from CCI- and SNL-injured DRG neurons 14 d after injury. The plots show the average percentage of neurons that responded to the applications of pharmacological ligands. ACh, 1 mM acetylcholine; AITC, 100 μM allyl isothiocyanate; ATP, 20 μM ATP; BR, 10 μM bradykinin; C, 500 nM capsaicin; ME, 400 μM Menthol. *A* compares neurons from injured with uninjured DRG post-CCI, and the percentage of ATP and bradykinin-responsive neurons are significantly higher compared to controls (explained in main text), whereas the percentage of acetylcholine- and capsaicin-responsive neurons were decreased. The number of neurons and number of trials compared were: ipsilateral CCI = 5,035 neurons from 33 trials, contralateral CCI = 4,519 neurons from 29 trials, ipsilateral sham = 2,176 neurons from 21 trials, contralateral sham = 2,028 neurons from 17 trials. The data were obtained from 13 CCI-operated and 11 sham-operated rats. *B* summarizes the average percentage of neurons that responded to the application of pharmacological ligands in SNL-injured DRG compared to uninjured DRGs. The neurons responsive to bradykinin and ATP were significantly increased after SNL injury, and the acetylcholine- and capsaicin-responsive neurons were significantly lower compared to uninjured DRG neurons. The number of neurons and trials compared were: ipsilateral SNL L5L6 = 1,028 neurons from five trials, contralateral SNL L5L6 = 960 neurons from five trials, sham ipsilateral L5L6 = 714 neurons from four trials, sham contralateral L5L6 = 277 neurons from two trials. The data were obtained from five SNL-operated rats and four sham-operated rats. $*P < 0.05$, $**P < 0.01$, $***P < 0.001$ obtained from nested logistical regression analysis. No significant differences were observed between injured contralateral and sham-operated groups.

Tracking Molecular Changes with the Progression to Neuropathic Pain States. To identify the earliest molecular changes that appear following nerve injury, SNL injured rats were behaviorally monitored at days 1, 3, 6, and 14 after injury as shown in Fig. 2. The numbers of acetylcholine-responsive neurons significantly decreased in SNL-injured DRG at day 1 (11± 2% of the total neurons, $P < 0.001$) compared to controls (33 ± 4% of total neurons), which was sustained through day 14. In addition, there was a significant increase in ATP responsive neurons (75 ± 2% of total neurons, $P < 0.001$) in SNL-injured DRG at day 1 compared to controls (44 ± 4% of the total neurons). The percentage of ATP-responsive neurons remained high throughout day 14. The number of capsaicin-responsive neurons began to decline

starting day 3 and continued to decrease until day 14. Progressive increase in bradykinin-responsive neurons were observed at days 3, 6, and 14 (see Fig. 4). No consistent change in response to menthol or allyl isothiocyanate (AITC) administration was detected. Thus, we monitored the molecular changes that appeared with the progression of pain states and the resulting effects in bradykinin-responsive neuronal phenotypes.

Behavioral Studies following CCI and SNL Nerve Injury. To observe correlations between molecular changes with pain behavior, we performed behavioral studies prior to extracting DRGs for constellation pharmacology experiments. *SI Appendix*, Fig. S1 shows the results of behavioral assays performed on rats following CCI and SNL nerve injury. Significant differences in pain behavior were observed 14-d postinjury, and this time point was set to capture changes at molecular level (10–14). As shown in *SI Appendix*, Fig. S1*A*, the rats display higher sensitivity to cold with increased frequency of paw withdrawal (*SI Appendix*, Fig. S1*A*) and increased duration of withdrawal events (*SI Appendix*, Fig. S1*B*) following CCI injury. In SNL-injured rats, tactile allodynia and thermal hyperalgesia were observed following injury. The threshold to thermal stimulus decreased in injured rats compared to the baseline scores obtained before the injury and to sham-operated rats (*SI Appendix*, Fig. S1*C*). Similarly, the withdrawal threshold to mechanical sensitivity also decreased significantly compared to scores before injury and to sham-operated animals (*SI Appendix*, Fig. S1*D*) ($P < 0.05$ for all behavioral studies).

Additionally, we performed behavioral assays and constellation pharmacology experiments on injured DRGs at different time points following SNL injury to identify the behavioral and molecular changes with the progression of pain states. As shown in *SI Appendix*, Fig. S2*A*, the SNL-injured rats display progressive reduction in thresholds to mechanical stimulus (*SI Appendix*, Fig. S2*A*) and heat stimulus (*SI Appendix*, Fig. S2*B*) starting at 3, 6, and 14 d post-SNL injury. These scores were compared with sham-operated rats and baseline scores prior to nerve injury. As shown in *SI Appendix*, Fig. S2, rats do not display any allodynia on day 1, but begin to develop tactile allodynia ($P < 0.05$) and thermal hyperalgesia ($P < 0.001$) on day 3 following injury.

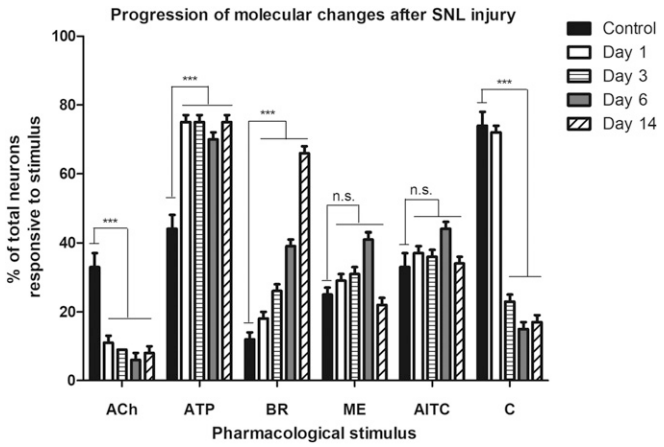

Fig. 2. Monitoring molecular changes with the progression of neuropathic pain induced by SNL injury. SNL injury induced molecular changes at days 1, 3, 6, and 14 after injury. The earliest changes were observed in the frequency of neurons responsive to acetylcholine and ATP. Only 11 ± 2% of total neurons obtained from injured DRG were responsive to ACh compared to 33 ± 4% in uninjured DRGs (controls) on day 1 following SNL injury. The bradykinin-responsive neurons progressively increased starting at day 3 and significantly increased to 66 ± 4% at day 14 post-SNL injury. *$P < 0.05$; **$P < 0.01$; ***$P < 0.001$; ns, not significant obtained from Fisher's exact test comparing the ipsilateral DRG neurons to contralateral DRG neurons from the same animal at each time point.

Coordinated Changes in Three Different Receptors Based on the Magnitude of Responses to Ligand Application. In addition to monitoring the frequency of responses, the magnitudes of calcium responses were also assessed. An example of coordinated changes associated with the increased responsiveness to bradykinin emerged through the analysis of the neurons that responded to both ATP and acetylcholine (*SI Appendix*, Fig. S4). *SI Appendix*, Fig. S4*A* shows phenotypic calcium-imaging traces of neurons from ipsilateral CCI DRGs that were responsive to both acetylcholine and ATP. *SI Appendix*, Fig. S4*C* shows similar traces from ipsilateral SNL DRGs. These have been sorted further into two groups: those that also responded to bradykinin and those that did not. We observed that in the neurons that responded to bradykinin, the calcium transient in response to ATP was generally greater than the calcium transient in response to acetylcholine. However, in the class of neurons that did not respond to bradykinin, the converse was usually true. This relationship is illustrated using a log plot as shown in *SI Appendix*, Fig. S4*B* and *SI Appendix*, Fig. S4*D*. The plot shows the logarithm of the ratio of the magnitude of responses of acetylcholine to ATP in each cell. In the controls, the responses to acetylcholine are commonly greater than the responses to ATP. In addition, the plot demonstrates that there is a leftward shift of the curve associated with ipsilateral CCI, suggesting that a significant proportion of neurons that responded to both acetylcholine and ATP now exhibit a larger magnitude of response to ATP than to acetylcholine. This effect is more pronounced in ipsilateral SNL cultures, as shown in *SI Appendix*, Fig. S4*D*. In contralateral CCI, 28% of these neurons (gray arrow) had higher ATP magnitude than acetylcholine and the majority of neurons (72%) had higher magnitude of acetylcholine than ATP. In ipsilateral CCI, an increased percentage of neurons (39%) had an ATP response magnitude that was greater than acetylcholine and the majority of these neurons were responsive to bradykinin. Thus, in the cluster of neurons represented to the left of the vertical line in *SI Appendix*, Fig. S4*B*, there are coordinated changes compared to the controls: (*i*) The response to ATP became greater than the response to acetylcholine (not observed in most control neurons), and (*ii*) a high proportion of neurons with an acetylcholine/ATP response <1 became responsive to bradykinin. Thus, the constellation of functional ion channels and receptors was altered in three different receptors and ion channels to yield the distinctive pharmacological profile found in a subset of ipsilateral DRG neurons.

In SNL cultures, the same trends were also evident and more pronounced. Only 29% of the neurons had acetylcholine responses greater than ATP responses, whereas in contralateral SNL cultures, 93% of the neurons had a phenotype where ACh magnitude was greater than ATP magnitude. Thus, DRG neurons from ipsilateral SNL exhibit profound concerted changes in receptor expression: significant up-regulation of ATP receptors and down-regulation of ACh receptors, accompanied by new expression of bradykinin receptors in the same neurons.

Grouping DRG Neurons Based on Phenotypic Calcium Profiles. In the experiments summarized in Fig. 1, the frequency of neurons responding to bradykinin in all of the control groups was similar (~12 ± 2%). In contrast, the frequency of bradykinin-responsive neurons obtained from injured DRG was approximately twofold higher in ipsilateral CCI (34 ± 2%) and fivefold higher in ipsilateral SNL L5L6 (66 ± 2%). Although the frequency of cells responding to bradykinin varied from experiment to experiment, the ipsilateral DRG neurons from CCI and SNL consistently showed a significant increase ($P < 0.001$) compared to contralateral DRG neurons in all experiments on animals that displayed chronic pain states in behavioral assays.

To obtain a more detailed understanding of changes taking place in different neuronal populations, we performed a parallel analysis of the data by classifying cells into subclasses based on their particular pharmacological profile as shown in Fig. 3. The bradykinin-responsive neurons could be categorized in five groups based on their responses to the application of other pharmacological agents and their frequency of occurrence is summarized in Fig. 4. There were additional (~8%) bradykinin-responsive neurons that appeared in SNL ipsilateral L5L6 cultures in addition to the five definite groups, and these have not been grouped as they constitute an overly heterogeneous assemblage, making them difficult to unequivocally categorize.

Group 1 neurons, in addition to responding to bradykinin, also responded to both menthol and capsaicin. Furthermore, the response of these neurons to AITC was very robust. In contrast, group 2 neurons did not respond to menthol but uniformly responded to capsaicin. There was heterogeneity in their response to AITC, but the response was not robust, if it occurs. These two groups appear to be canonical bradykinin-responsive neurons and were observed in all cell cultures as indicated in Fig. 4. Groups 3–5 neurons were absent in control cultures from CCI and SNL and appeared only in cultures of injured DRG (ipsilateral CCI and ipsilateral SNL L5L6). Thus, the appearance of three new phenotypic groups of bradykinin-responsive neurons with distinctive pharmacological profiles contributed toward the majority of increase in bradykinin responses shown in Fig. 1. Group 3 neurons responded to ATP and bradykinin only and contributed toward an 11% increase in bradykinin responses from ipsilateral CCI culture and 30% increase in ipsilateral SNL L5L6 (shown in Fig. 4*A*). Group 4 neurons were defined based on their magnitude of response to acetylcholine and ATP. In this group, the magnitude of ATP responses was higher than acetylcholine and they generally responded to the application of AITC. Similar to group 3, these neurons appeared only in ipsilateral CCI and SNL L5L6 and were absent in all controls. The pharmacological profile of group 5 is a hybrid between groups 3 and 4. Unlike group 4 neurons, these did not respond to acetylcholine, but like group 4 neurons, responded to ATP and to AITC. They differed from the group 3 neurons that uniformly did not respond to the application of AITC.

Thus, groups 1 and 2 are more canonical neurons that may include polymodal peptidergic nociceptors found in controls, ipsilateral CCI and ipsilateral SNL L5L6. The CCI and SNL injury result in the appearance of three new groups that are shown in Fig. 3 (groups 3–5).

In addition, the incremental increase in bradykinin responsive neurons that was observed at 3, 6, and 14-d post injury (Fig. 2) were phenotypically assessed and the progressive increase in bradykinin responses appeared from the new cellular phenotypes described above (Fig. 3, groups 3–5). The quantitative analysis of these phenotypes, as shown in Fig. 4*B*, demonstrate that the new bradykinin responsive neurons are absent at day 1 following injury and begin to appear and increase starting day 3 postinjury.

Tracking DRG Cell Classes after Nerve Injury. Tandem immunostaining after constellation pharmacology experiments were performed. The cells were stained with isolectin B4 (shown in red, IB4 conjugated with Alexa 564 dye) to identify nonpeptidergic nociceptors and an antibody for calcitonin gene-related peptide (CGRP, shown in green, secondary antibody conjugated with Alexa 488 dye) to identify peptidergic nociceptors. In neurons subjected to CCI, the percentages of IB4- and CGRP-stained neurons were reduced and nearly absent 14-d post-nerve injury (shown in *SI Appendix*, Fig. S4). It is also notable that the majority of the $IB4^{-}$ $CGRP^{-}$ neurons in control DRG were capsaicin responsive, and a significant fraction of these cells did not respond to capsaicin in the ipsilateral CCI and ipsilateral SNL L5L6 DRG. These results are suggestive of coordinated, multivalent changes in ATP, bradykinin, and capsaicin receptors in a subset of DRG neurons. We monitored the calcium responses from these two groups of neurons at different time points after nerve injury.

Signature calcium traces from these two groups are shown in Fig. 5. Uninjured nonpeptidergic neurons that express nAChRs generally do not respond to the application of ATP. 1 d post-SNL injury, these neurons display an up-regulation of ATP responses (Fig. 5*B*). In contrast, no significant changes in ATP or bradykinin responses were observed in peptidergic neurons 1-d post-SNL injury. Although the number of IB4+ neurons gradually decrease after nerve injury, we were able to track the IB4+ nAChR-expressing neurons up to 3-d post-nerve injury. We previously compared mouse and rat DRG neurons (15) and predict that the ACh+ IB4+ cells are a subset of broad clusters viz. NP1-NP3, as described by Usoskin et al., and the CGRP+ cells are a subset of Pep1/Pep2 clusters (16, 17). Based on our previous work, we conclude alpha6/alpha3 nicotinic receptors in these neuronal groups are down-regulated after nerve injury. Loss of alpha6 nicotinic receptors have been shown to increase pain responses (18) and, thus, the loss of nicotinic receptors in these two groups of nonpeptidergic neurons can be relevant to the establishment of chronic pain states. The bradykinin responsive cell groups were analyzed for these stains. Group 1 and group 2 neurons were largely positive for CGRP in controls. In contrast, the cell groups that appear in ipsilateral CCI and ipsilateral SNL L5L6 cultures (groups 3–5, Fig. 5) were negative to both IB4 and CGRP stains. These staining data suggest that multivalent molecular changes occur in different cell types (including unlabeled cells, IB4+ cells, and CGRP+ cells) that result in convergence to new bradykinin responsive neuronal phenotypes.

Discussion

We analyzed functional phenotypic changes that occur in DRG neurons when a pathological chronic pain state is triggered in two animal models of nerve injury, CCI and SNL. Neurons from the ipsilateral lumbar DRG from CCI and SNL were compared to multiple controls, including neurons from the contralateral DRGs of the same animal and from ipsilateral and contralateral DRGs from sham-operated animals. There were no significant differences observed between the three control DRG cultures. In contrast, significant differences were uncovered when neurons from ipsilateral DRG of CCI/SNL rats were compared to controls. A particularly notable observation was the increase in the fraction of DRG neurons that responded to bradykinin (Fig. 1). This increase was due to the appearance of three distinctive neuronal subclasses (Fig. 3). One neuronal subclass responded to bradykinin and ATP. The DRG neurons that share this profile accounted for approximately half of the observed increase in the overall frequency of neurons responding to bradykinin (Fig. 4*A*). In addition to changes in the frequency of bradykinin responsive neurons, the magnitudes of calcium response in these groups were also altered. As an example, the magnitude of Ach- and ATP-elicited calcium signals were significantly different between injured and uninjured groups as shown in *SI Appendix*, Fig. S3. Similar analysis for other members of the constellations such as bradykinin, AITC, and capsaicin are underway, which can potentially advance our understanding of the receptor interactions in shaping cellular physiology.

Other subsets of neurons with a pharmacological profile found only in the experimental neurons (from ipsilateral DRGs in CCI and SNL rats) are illustrated in Fig. 3 as groups 4 and 5. The group 5 phenotype appears to represent a subset of the group 4 neurons that have lost their responsiveness to ACh completely. Together, groups 3, 4, and 5 account for the majority of increase in the frequency of DRG neurons that respond to bradykinin in

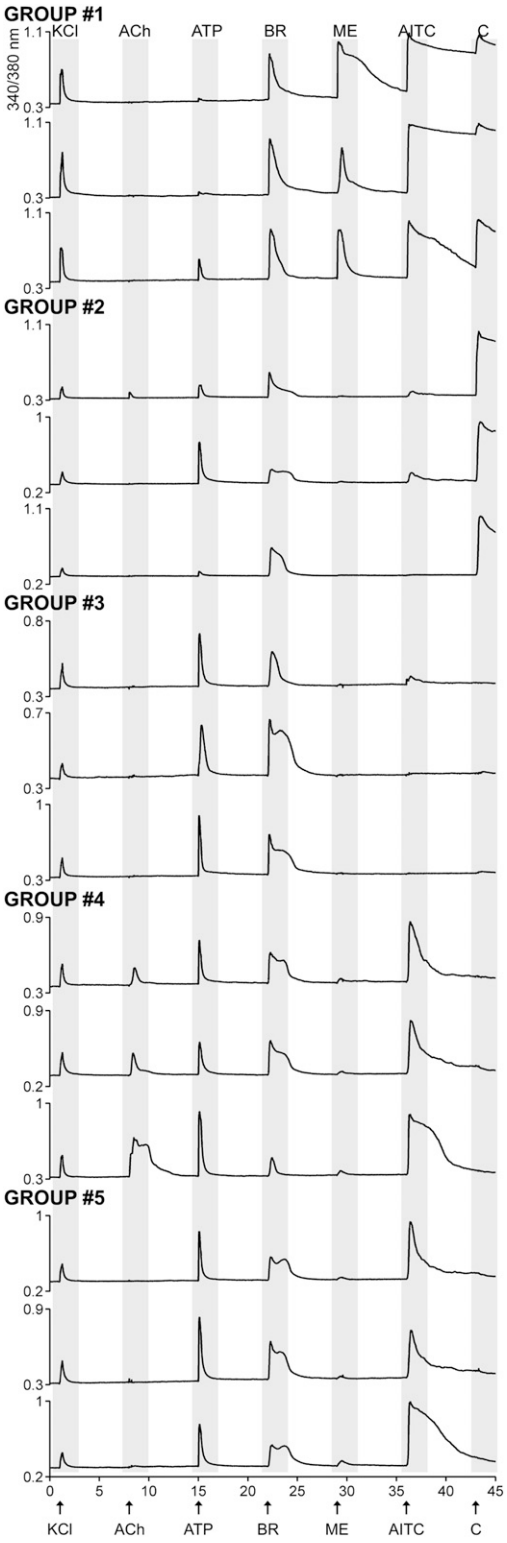

Fig. 3. New bradykinin-responsive neuronal phenotypes appear following CCI and SNL injury. The bradykinin-responsive neurons were categorized into five phenotypic groups based on their calcium response phenotypes to the application of pharmacological ligands. Each calcium-imaging trace is a representative response profile from a single neuron within the group. Group 1 and group 2 are bradykinin-responsive neurons that responded to capsaicin. Group 1 neurons responded to menthol, whereas group 2 neurons did not. Groups 3–5 are bradykinin-responsive neurons that were insensitive to capsaicin. Neuronal profiles shown in groups 3–5 were found only in injured DRG neurons (ipsilateral CCI and ipsilateral SNL L5L6 cultures) and were absent in uninjured DRG (controls). *x* axis (time in minutes): sequential application of pharmacological ligands monitored over an hour. Arrows indicate 15-s application of the following: ACh, 1 mM acetylcholine; AITC, 100 μM allyl isothiocyanate; ATP, 20 μM ATP; BR, 10 μM bradykinin; C, 500 nM capsaicin; KCl, 30 mM potassium chloride; ME, 400 μM Menthol. *y* axis: ratio of 340 nM/380 nM, is a measure of intracellular calcium levels.

the ipsilateral CCI and SNL DRGs, are only found in injured DRG, and were absent in uninjured DRG.

The properties of nociceptive neurons change, as evidenced by the loss of IB4 binding and/or CGRP expression observed by our immunostaining data as well as previously published results (19), in addition to other changes in receptor and ion channel expression, such as TRPV1. The significant decrease in capsaicin-responsive neurons suggests that TRPV1 expression is decreased following CCI and SNL injury in rats. It is unclear how the reduction in capsaicin-responsive neurons could lead to pain states as TRPV1 has been conventionally associated with nociception, although TRPV1 receptor itself may not directly mediate the pain signal (20); this observation will require investigation of constellations of other receptors within the TRPV1-expressing neurons that could provide insight into how these combinatorial changes might be correlated to a physiologically relevant neuropathic pain state. Notably, ∼70% of the uninjured rat DRG neurons respond to the application of capsaicin (Fig. 1), and the reduction in capsaicin responses were observed in the IB4-CGRP- neurons, which can belong to large diameter mechanosensitive class and/or to small diameter C-LTMRs. Presumably, the changes observed in neurons from injured DRG (ipsilateral CCI and SNL) may arise as a result of phenotypic changes in previously nonnociceptive neurons, which begin to express nociceptive markers such as the up-regulated expression of bradykinin and ATP receptors, which warrants further investigation.

We specifically monitored molecular changes in two groups of neurons: CGRP-expressing peptidergic neurons and IB4-binding nonpeptidergic neurons. nAChR expressing nonpeptidergic neurons display significant up-regulation of ATP receptors 1 d post-SNL injury, whereas peptidergic neurons did not display significant changes on day 1 postinjury. To monitor the earliest molecular events that occur following nerve injury, we performed a series of experiments at days 1, 3, 6, and 14 following SNL injury. As shown in *SI Appendix*, Fig. S2, the behavioral tests to assess the thresholds for tactile and thermal sensitivity reduced starting at day 3 postnerve injury. The corresponding molecular changes are shown in Fig. 2. As shown, at day 1 following nerve injury, the pain scores of animals tested were similar to sham-operated rats, but some molecular changes already began to appear, with a decrease in Ach-responsive neurons and an increase in ATP-responsive neurons. The coordinated changes in ACh, ATP, bradykinin, and capsaicin are illustrated in Figs. 3 and 5.

A major question that arises is whether the appearance of the new phenotypes contributes toward neuropathic pain (or do some of these appear as a result of the nerve injury?). Further investigations can clarify this by: (*i*) testing pharmacological interventions that alleviate chronic pain and observing their effects on the appearance of these aberrant neuronal phenotypes, and (*ii*) using a mixture of pharmacological blockers of ATP and bradykinin receptors and observe the effect on rat behavior following nerve injury. Thus, the current work opens avenues to explore chronic pain studies, at cellular and molecular levels. In this study, we have made it straightforward to define functional changes in receptor and ion channel expression that result in the appearance of neuronal phenotypes. Identification of cell types and monitoring cell-specific changes with disease progression is the first step in addressing physiological changes underlying pathological conditions. For example, future studies aimed at

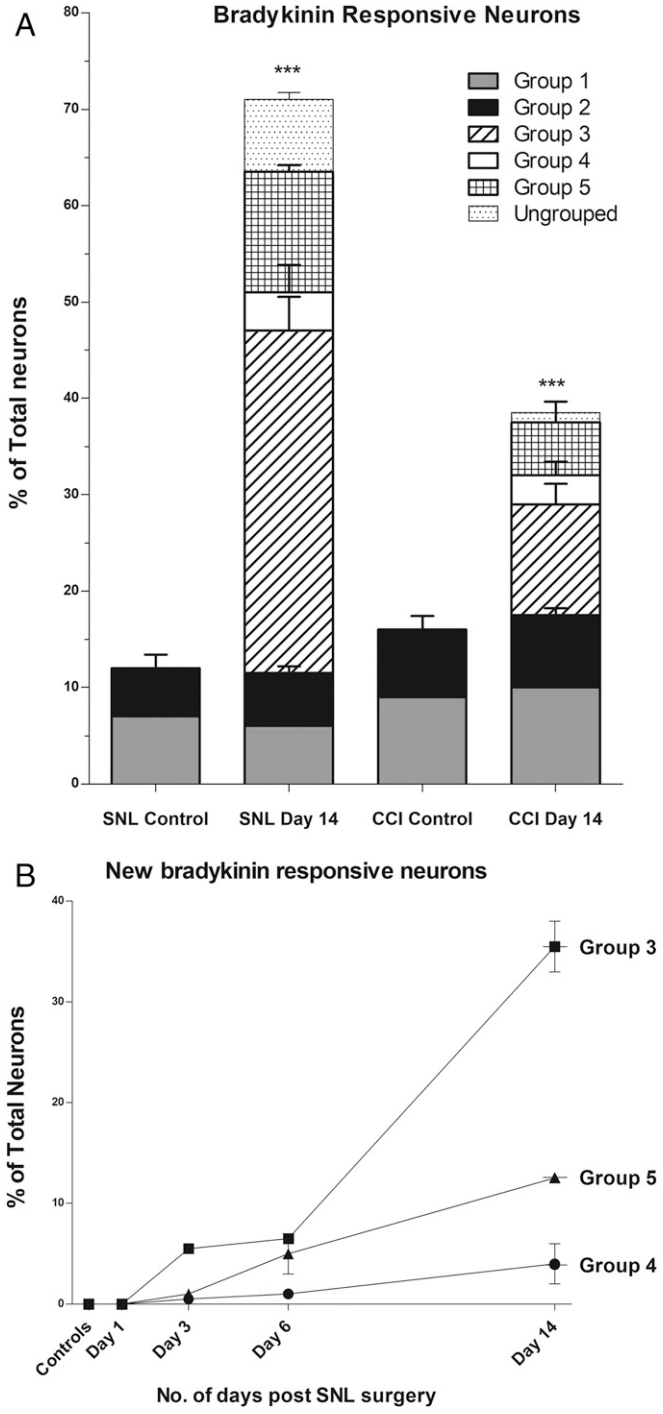

Fig. 4. Quantitative analysis of bradykinin-responsive neuronal phenotypes. (*A*) Quantifying the appearance of new bradykinin-responsive neurons in CCI and SNL DRGs. The phenotypic profiles of bradykinin-responsive neuronal groups shown in Fig. 3 were quantified. Groups 1 and 2 were found in all trials (injured experimental trials and uninjured control trials) and accounted for 12 ± 2% of the total neurons. In CCI- and SNL-injured DRG neurons, the net increase in bradykinin-responsive neurons found 14 d postinjury was accounted by the appearance of new phenotypes as shown in Fig. 3 (groups 3–5). Group 3 appeared with a frequency of 32 ± 2% in the ipsilateral SNL L5L6 and 9% in the ipsilateral CCI. Groups 4 and 5 also appeared only in the injured SNL DRGs (4 ± 2% and 11 ± 2%, respectively) and CCI-injured DRG (3 ± 1% and 5 ± 1%, respectively) and were absent in uninjured DRG. *y* axis: percentage of total neurons with phenotypic profiles shown in Fig. 5; *x* axis: type of DRG tissue 14-d postsurgery. (*B*) Tracking the appearance of new bradykinin-responsive neuronal phenotypes in SNL DRGs with the progression of neuropathic pain: The new bradykinin-responsive neuronal groups (shown in Fig. 3, groups 3–5) did not appear on day 1 and started to appear at day 3, further up-regulated at days 6 and 14 after SNL injury. The progressive increase in bradykinin-responsive neurons is accounted by the appearance of new bradykinin-responsive neuronal groups as shown here. $*P < 0.05$, $**P < 0.01$, $***P < 0.001$ obtained from nested logistical regression analysis.

recording cellular responses to the application of cold temperature solutions from cell types identified in this work can help uncover relevant cellular mechanisms that underlie cold allodynia. The availability of transgenic mouse lines labeling different cell types will strengthen the ability to track changes in different cell types following nerve injury. However, the approach described in this work can be used to monitor cellular and molecular changes in pathological states in other animal models of disease, even when transgenic animals are not readily available and allows for comparative analysis across different species to identify common molecular changes relevant to pathology.

Although valuable, the whole DRG transcriptomic approach provides only limited information on the differential dysregulation of genes (5, 21). By tracking the coordinated changes in membrane constellations within individual neuronal groups, an approach to investigate pathology at the systems and molecular level in a defined cell-specific manner becomes feasible, as illustrated by *SI Appendix*, Fig. S5. SNL-induced molecular changes were tracked in 16 cell types of sensory neurons (identified by constellation pharmacology). An example of one subset of nonpeptidergic neurons (identified by IB4 stain) is shown, and the representative intracellular calcium profiles from two individual neurons from this group are represented at different time points after nerve injury. As shown, the uninjured neurons in this group have a bright ring stain and respond to the application of high $[K^+]_o$ and 300 nM capsaicin. After the nerve injury, the neurons in this group begin to respond to the application of ATP 1 d postinjury and bradykinin 3 d postinjury, while gradual loss of the response to capsaicin and IB4 stain was observed by 14 d postinjury. This demonstrates our ability to track changes to the receptor constellations in different cell types with the progression of pathology. Thus, simultaneous multivalent changes occurring in each cell type during the progression of pathology can be tracked using this approach. We refer to this approach as the "Pigafetta Chronicles of Pathology," named after Italian explorer Antonio Pigafetta, whose meticulous cartographic notes during Magellan's voyage of discovery around the globe proved extremely valuable to the future explorers. Monitoring changes in the cell type-specific receptor constellations with disease progression is a crucial step in the discovery of disease relevant molecular targets and the development of novel therapeutics that can prevent the progression of the disease, not just alleviate the symptoms.

Material and Methods

A detailed description of materials and methods can be found in *SI Appendix*.

Animals. Adult, male Sprague–Dawley rats (200–250 g at the time of surgery, Envigo) were used. All procedures were performed in accordance with the guidelines of the Committee for Research and Ethical Issues of the International Association for the Study of Pain (IASP) under protocols approved by the University of Arizona and University of Utah Institutional Animal Care and Use Committee. Rats were housed on a 12-h light-dark cycle with food and water ad libitum.

Surgeries.

CCI. CCI surgeries were done according to the description of Bennet et al., (22). Briefly, rats were anesthetized with 5% isofluorane in air at 1 L/min and maintained with 2.5% isofluorane. The sciatic nerve was exposed at

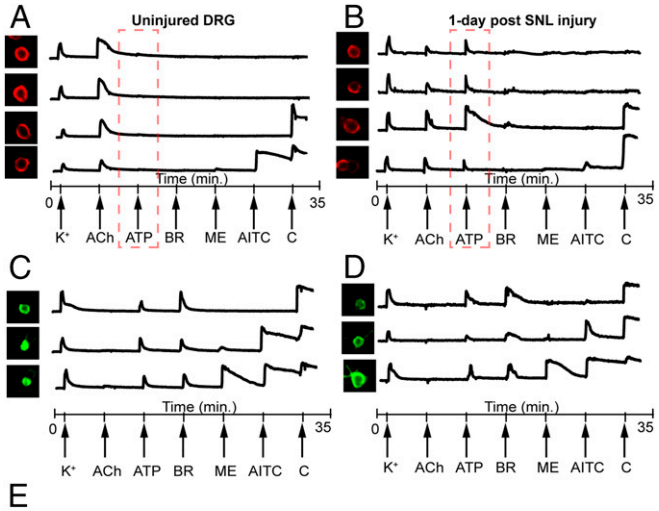

Days post-injury	DRG type	Total Neurons	# of Neurons (% of Total Neurons)			
			CGRP+	ATP+/BR+	IB4+	ATP+/BR+
Day 1	Contralateral L5L6	1109	206 (19%)	113 (10%)	893 (81%)	133 (12%)
Day 1	Ipsilateral L5L6	855	164 (19%)	106 (12%)	517(60%)	259 **(30%)**

Fig. 5. Monitoring changes to receptor constellations in different cell types. Representative calcium imaging traces from nAChR expressing IB4+ nonpeptideric neurons from uninjured DRG (*A*), nAChR expressing IB4+ nonpeptideric neurons from injured DRG 1-d post SNL (*B*), CGRP-expressing peptidergic neurons from uninjured DRG (*C*), and CGRP-expressing peptidergic neurons from injured DRG 1-d post SNL injury (*D*). (*E*) ATP or bradykinin responsive neurons in the four groups (*A*–*D*) were quantified and significant increase in ATP responses were observed in a subset of nonpeptidergic neurons.

midthigh level. Four loose ligatures using 4–0 chromic gut suture were placed around the exposed sciatic nerve about 2 mm apart. Sham-operated animals underwent the same procedure but without the ligatures to the sciatic nerve.

SNL. The surgical procedure for L5/L6 SNL was performed according to Kim and Chung (3). Briefly, anesthesia was induced with 5% and maintained with 2.5% isofluorane in air. A 2-cm midline incision was made and the lumbar 5 and 6 spinal nerves (L5/L6) were exposed and tightly ligated with 4–0 silk suture. The incision was closed, and the animals were returned to their home cages. Sham-operated control rats were prepared in an identical manner except that the L5/L6 spinal nerves were not ligated.

Behavioral Assays. The detailed description of behavioral assays can be found in *SI Appendix, Materials and Methods*. The pain state of the animals was assessed by different behavioral tests. For CCI, animals were assessed for the development of cold allodynia. Animals subjected to SNL injury were observed for tactile allodynia and thermal hyperalgesia.

The animals were assessed for the development of cold allodynia, tactile allodynia, mechanical, and thermal hyperalgesia by using previously described methods (23–28).

Calcium Imaging on Dissociated Neurons. Two weeks after the surgeries, the lumbar DRG of all animals were dissected. For CCI trials, DRG from L4–L6 from the following groups were analyzed: ipsilateral side and contralateral side of experimental and sham-operated control animals. For SNL trials, L5–L6 DRGs from the ipsilateral and contralateral side of experimental and sham-operated control animals were analyzed separately from L4 DRG. The tissues were stored separately in cell culture medium and shipped on ice overnight. DRGs were kept on ice, transferred to a tissue culture-treated (by vacuum gas plasma) Petri dish (BD Biosciences) with HBSS (ThermoFisher, catalog no. 14175103) and cleaned to remove debris and excessive tissue. A series of control experiments were performed at the University of Arizona to assess and eliminate variations arising from shipping procedure.

The details of obtaining cell culture for calcium imaging experiments DRGs are explained in *SI Appendix, Materials and Methods*. Briefly, DRGs were incubated with trypsin for 18 min in water bath at 37 °C, followed by mechanical trituration and centrifugation to obtain dense cell pellet. The pellets were resuspended in cell culture medium, plated on a poly-lysine–coated 24-well tissue culture plate (BD Biosciences) and kept in an incubator overnight at 37 °C supplied with 5% CO_2. Cells were loaded with 2.5 μM FURA-2-AM (ThermoFisher, catalog no. F-1221) and kept for an hour in the incubator before calcium imaging experiments. The recipe for cell culture media, bath solutions, and ligand concentrations are detailed in *SI Appendix, Materials and Methods*.

Immunostaining. Immunostaining was performed in tandem with calcium imaging experiments. The field of view was identified based on the *x-y* coordinates on microscope stage. After calcium imaging experiments, plates were taken out for immunostaining protocols. Briefly, cells were fixed using 4% paraformaldehyde, permeabilized using 0.25% Triton-X-100, blocked with 10% donkey serum (Jackson Immunoresearch catalog no. 017-000-121) and 30 mM glycine. Anti-CGRP primary antibody (1:2,000 dilution, Immunostar catalog no. 24112) in 0.1% donkey serum was added to the wells, and the cells were incubated with primary antibody overnight at 4 °C on a shaker. The primary antibody was aspirated, and cells were washed three times with ice-cold saline. One milliliter of secondary antibody (1:200 dilution, Thermofisher catalog no. A-21206) was added and cells were incubated with secondary antibody for 1 h at room temperature on a shaker. Fluorescent images were captured from the same field of view as identified and realigned by appropriate positioning of the *x-y* coordinates on microscope stage.

Data Analysis. The responses to the application of ligands were also scored manually in a binary format (0 or 1 for absence and increase of calcium influx, respectively). The baseline calcium level for each cell trace was observed, and a response was assigned as positive calcium influx (value = 1), if the magnitude of calcium influx was higher than a threshold of 0.05 units (of 340/380 ratio) above the baseline. In addition, the time course of the 340:380 ratio for each regions of interest (ROI [trace]) was analyzed using a set of R functions (R Core Team 2013) for quantitative analysis of peak heights, clustering, and determination of cell-phenotype percentages as described previously (29).

Data Availability. All study data are included in the article and supporting information.

ACKNOWLEDGMENTS. We thank Dr. Jeff Woodbury for helpful comments and discussions in drafting the manuscript. We also thank Dr. Rajesh Khanna for providing resources to complete experiments at The University of Arizona. This work was supported by Department of Defense PR Grant 161686, "Novel strategies for accelerating non-opioid drug discovery," and National Institute of General Medical Sciences Grant GM 48677, "*Conus* Peptides and Their Receptor Targets: Towards Constellation Pharmacology" (to B.M.O.). This work is based in part on the PhD dissertation of S.R.

1. R. W. Teichert, E. W. Schmidt, B. M. Olivera, Constellation pharmacology: A new paradigm for drug discovery. *Annu. Rev. Pharmacol. Toxicol.* **55**, 573–589 (2015).
2. Y. Zheng *et al.*, Deep sequencing of somatosensory neurons reveals molecular determinants of intrinsic physiological properties. *Neuron* **103**, 598–616.e7 (2019).
3. S. H. Kim, J. M. Chung, An experimental model for peripheral neuropathy produced by segmental spinal nerve ligation in the rat. *Pain* **50**, 355–363 (1992).
4. I. Decosterd, C. J. Woolf, Spared nerve injury: An animal model of persistent peripheral neuropathic pain. *Pain* **87**, 149–158 (2000).
5. M. A. Bangash *et al.*, Distinct transcriptional responses of mouse sensory neurons in models of human chronic pain conditions. *Wellcome Open Res.* **3**, 78 (2018).
6. G. Petho, P. W. Reeh, Sensory and signaling mechanisms of bradykinin, eicosanoids, platelet-activating factor, and nitric oxide in peripheral nociceptors. *Physiol. Rev.* **92**, 1699–1775 (2012).
7. G. R. Dubé *et al.*, Loss of functional neuronal nicotinic receptors in dorsal root ganglion neurons in a rat model of neuropathic pain. *Neurosci. Lett.* **376**, 29–34 (2005).
8. D. Levy, D. W. Zochodne, Increased mRNA expression of the B1 and B2 bradykinin receptors and antinociceptive effects of their antagonists in an animal model of neuropathic pain. *Pain* **86**, 265–271 (2000).
9. A. J. Hone, J. M. McIntosh, Nicotinic acetylcholine receptors in neuropathic and inflammatory pain. *FEBS Lett.* **592**, 1045–1062 (2018).
10. Y. L. Kuo *et al.*, K^+ channel modulatory subunits KChIP and DPP participate in Kv4-mediated mechanical pain control. *J. Neurosci.* **37**, 4391–4404 (2017).
11. L. Blaszczyk *et al.*, Sequential alteration of microglia and astrocytes in the rat thalamus following spinal nerve ligation. *J. Neuroinflammation* **15**, 349 (2018).
12. F. Denk, M. Crow, A. Didangelos, D. M. Lopes, S. B. McMahon, Persistent alterations in microglial enhancers in a model of chronic pain. *Cell Rep.* **15**, 1771–1781 (2016).

13. C. Zhu, Q. Xu, C. Wang, Z. Mao, N. Lin, Evidence that CA3 is underling the comorbidity between pain and depression and the Co-curation by Wu-Tou decoction in neuropathic pain. *Sci. Rep.* **7**, 11935 (2017).
14. R. Patel *et al*., Anti-hyperalgesic effects of a novel TRPM8 agonist in neuropathic rats: A comparison with topical menthol. *Pain* **155**, 2097–2107 (2014).
15. N. J. Smith *et al*., Comparative functional expression of nAChR subtypes in rodent DRG neurons. *Front. Cell. Neurosci.* **7**, 225 (2013).
16. D. Usoskin *et al*., Unbiased classification of sensory neuron types by large-scale single-cell RNA sequencing. *Nat. Neurosci.* **18**, 145–153 (2015).
17. M. Häring *et al*., Neuronal atlas of the dorsal horn defines its architecture and links sensory input to transcriptional cell types. *Nat. Neurosci.* **21**, 869–880 (2018).
18. J. S. Wieskopf *et al*., The nicotinic α6 subunit gene determines variability in chronic pain sensitivity via cross-inhibition of P2X2/3 receptors. *Sci. Transl. Med.* **7**, 287ra72 (2015).
19. R. Ruscheweyh, L. Forsthuber, D. Schoffnegger, J. Sandkühler, Modification of classical neurochemical markers in identified primary afferent neurons with Abeta-, Adelta-, and C-fibers after chronic constriction injury in mice. *J. Comp. Neurol.* **502**, 325–336 (2007).
20. D. A. Yarmolinsky *et al*., Coding and plasticity in the mammalian thermosensory system. *Neuron* **92**, 1079–1092 (2016).
21. H.-S. Xiao *et al*., Identification of gene expression profile of dorsal root ganglion in the rat peripheral axotomy model of neuropathic pain. *Proc. Natl. Acad. Sci. U.S.A.* **99**, 8360–8365 (2002).
22. G. J. Bennett, Y. K. Xie, A peripheral mononeuropathy in rat that produces disorders of pain sensation like those seen in man. *Pain* **33**, 87–107 (1988).
23. L. O. Randall, J. J. Selitto, A method for measurement of analgesic activity on inflamed tissue. *Arch. Int. Pharmacodyn. Ther.* **111**, 409–419 (1957).
24. T. King *et al*., Unmasking the tonic-aversive state in neuropathic pain. *Nat. Neurosci.* **12**, 1364–1366 (2009).
25. S. R. Chaplan, F. W. Bach, J. W. Pogrel, J. M. Chung, T. L. Yaksh, Quantitative assessment of tactile allodynia in the rat paw. *J. Neurosci. Methods* **53**, 55–63 (1994).
26. W. J. Dixon, Efficient analysis of experimental observations. *Annu. Rev. Pharmacol. Toxicol.* **20**, 441–462 (1980).
27. C. Qu *et al*., Lesion of the rostral anterior cingulate cortex eliminates the aversiveness of spontaneous neuropathic pain following partial or complete axotomy. *Pain* **152**, 1641–1648 (2011).
28. S. E. Burgess *et al*., Time-dependent descending facilitation from the rostral ventromedial medulla maintains, but does not initiate, neuropathic pain. *J. Neurosci.* **22**, 5129–5136 (2002).
29. K. J. Curtice *et al*., Classifying neuronal subclasses of the cerebellum through constellation pharmacology. *J. Neurophysiol.* **115**, 1031–1042 (2016).